RESEARCH ARTICLE

Printing amphotericin B on microneedles using matrix-assisted pulsed laser evaporation

Roger Sachan[1], Panupong Jaipan[2], Jennifer Y. Zhang[3], Simone Degan[3], Detlev Erdmann[4], Jonathan Tedesco[5], Lyndsi Vanderwal[6], Shane J. Stafslien[6], Irina Negut[7], Anita Visan[7], Gabriela Dorcioman[7], Gabriel Socol[7], Rodica Cristescu[7], Douglas B. Chrisey[8] and Roger J. Narayan[2*]

[1] Wake Early College of Health and Sciences, Raleigh, North Carolina, USA
[2] Joint Department of Biomedical Engineering, The University of North Carolina and North Carolina State University, Raleigh, North Carolina, USA
[3] Department of Dermatology, Duke University Medical Center, Durham, North Carolina, USA
[4] Department of Surgery, Division of Plastic, Reconstructive, Maxillofacial and Oral Surgery, Duke University Medical Center, Durham, North Carolina, USA
[5] Keyence Corporation of America, Elmwood Park, New Jersey, USA
[6] Office of Research and Creativity Activity, North Dakota State University, 1715 Research Park Drive, Fargo ND, USA
[7] National Institute for Lasers, Plasma and Radiation Physics, Lasers Department, P.O. Box MG-36, Bucharest-Magurele, Romania
[8] Department of Physics and Engineering Physics, Tulane University, New Orleans, LA, USA

Abstract: Transdermal delivery of amphotericin B, a pharmacological agent with activity against fungi and parasitic protozoa, is a challenge since amphotericin B exhibits poor solubility in aqueous solutions at physiologic pH values. In this study, we have used a laser-based printing approach known as matrix-assisted pulsed laser evaporation to print amphotericin B on the surfaces of polyglycolic acid microneedles that were prepared using a combination of injection molding and drawing lithography. In a modified agar disk diffusion assay, the amphotericin B-loaded microneedles showed concentration-dependent activity against the yeast *Candida albicans*. The results of this study suggest that matrix-assisted pulsed laser evaporation may be used to print amphotericin B and other drugs that have complex solubility issues on the surfaces of microneedles.

Keywords: matrix-assisted pulsed laser evaporation, microneedle, amphotericin B, antifungal

*Correspondence to: Roger J. Narayan, UNC/NCSU Joint Department of Biomedical Engineering, Raleigh, NC 27695-7115, USA; Email: roger_narayan@unc.edu

Received: June 5, 2017; **Accepted**: July 3, 2017; **Published Online**: July 14, 2017

Citation: Sachan R, Jaipan P, Zhang J Y, *et al*., 2017, Printing amphotericin B on microneedles using matrix-assisted pulsed laser evaporation. *International Journal of Bioprinting*, vol.3(2): 147–157. http://dx.doi.org/10.18063/IJB.2017.02.004.

1. Introduction

Amphotericin B is a "gold standard" for the systemic treatment of fungal infections (*e.g.*, *Candida albicans* infections) as well as parasitic protozoal infections[1,2]. This polyene agent interacts with the ergosterol component of the fungal cell membrane, resulting in increased fungal cell membrane permeability and fungal cell death[3–5]. Amphotericin B exhibits renal toxicity; renal failure requiring hemodialysis is associated with the use of amphotericin B at high doses over a prolonged period[1,2]. Anemia, convulsions, hypertension, and tremors have also been associated with the use of amphotericin B[3–5]. Amphotericin B is commonly utilized for the treatment of fungal infections despite this significant side-effect profile because it exhibits the broadest antifungal spectrum, the most potent fungicidal activity, and the least likelihood for the generation of antimicrobial resistance among all antifungal agents[3–5].

One approach for minimizing the side effects associated with the use of amphotericin B for the treat-

ment of cutaneous fungal infections involves the use of transdermal drug delivery devices. Microneedles are 50 µm- to 1 mm-long lancet-shaped devices that may be used to directly deliver amphotericin B to the site of infection[6,7]. These devices are used to create pathways in the keratinized stratum corneum layer of the skin, which commonly prevents the movement of pharmacological agents through the skin[8]. Due to the small dimensions of microneedles, tissue damage at the treatment site is minimized. Microneedles are associated with low levels of pain since they do not penetrate deeper portions of the dermis layer of the skin, where many large nerve endings are found[9].

One of the challenges associated with developing novel amphotericin B drug delivery methods is that amphotericin B exhibits poor solubility in aqueous solutions at physiological pH values[1,2]. Amphotericin B exhibits amphipathic behavior because of the apolar and polar components of the lactone ring. Due to its amine and carboxyl groups, amphotericin B exhibits amphoteric behavior. As a result of these features, amphotericin B is insoluble in many organic solvents and aqueous solvents. Several formulations have been developed to reduce amphotericin B toxicity, such as methyl ester and lipid conjugate (*e.g.*, colloidal dispersion, lipid complex, and liposome) forms[3–5]. For example, several lipid-containing formulations, including microsphere formulations, nanosphere formulations, nanoparticle formulations, and nanodisk formulations, have been developed; these formulations exhibit reduced renal toxicity[3–5,10]. Unfortunately, many lipid-containing formulations are associated with much higher cost than conventional amphotericin B delivery methods.

In a previous paper, piezoelectric inkjet printing was used to deposit amphotericin B on the surfaces of Gantrez® 169 BF microneedles that were created using a combination with visible light dynamic mask microstereolithography and micromolding. The amphotericin B-loaded microneedles exhibited antifungal activity against the yeast *Candida parapsilosis*[11]. It should be noted that coating thickness in piezoelectric inkjet printing and many other conventional processes is not well controlled; for example, surface wetting may affect coating thickness[12,13].

In this paper, we printed amphotericin B onto the surfaces of polyglycolic acid microneedle arrays using matrix-assisted pulsed laser evaporation[14–18]. Matrix-assisted pulsed laser evaporation process involves laser ablation of a frozen target that contains an amount of diluted pharmacological agent in a volatile solvent[14–18]. The dimethyl sulfoxide solvent is relatively volatile, possesses a high vapor pressure, and preferentially absorbs the laser energy. The dimethyl sulfoxide molecules do not deposit on the substrate due to their low sticking coefficients. The amphotericin B molecules at the gas–matrix interface are ejected when kinetic energy is transferred during collisions with the solvent molecules. The less volatile amphotericin B molecules deposit on the substrate and form the vast majority of the coating.

Matrix-assisted pulsed laser evaporation enables the thickness of the coating that is printed on the surface of the microneedle to be tightly controlled (Figure 1)[19]. Matrix-assisted pulsed laser evaporation allows one to print a pharmacological agent with precise thickness control since it is a "line-of-sight" physical vapor

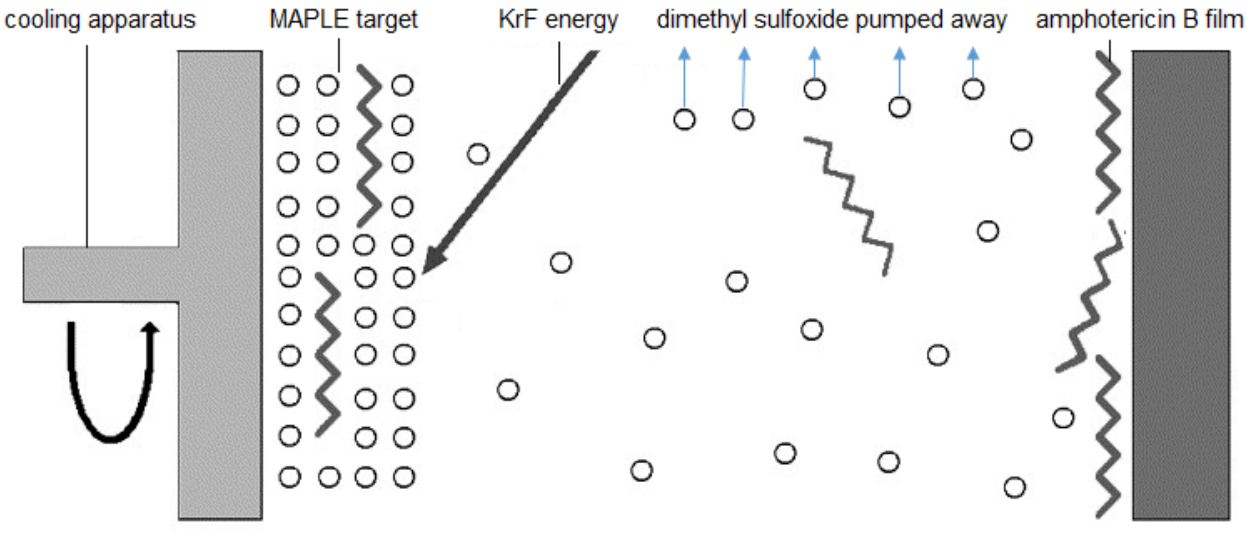

Figure 1. Schematic of the matrix-assisted pulsed laser evaporation process[19]. (Reprinted with permission from Elsevier.)

deposition approach. This approach also provides excellent control over coating roughness and coating homogeneity. Finally, matrix-assisted pulsed laser evaporation is a "cold coating process", since the depositing species are not heated.

Coatings containing several drugs, including gamma-cyclodextrin/usnic acid and gentamicin sulfate, have been deposited using matrix-assisted pulsed evaporation[19–21]. For example, poly(D,L-lactide)-gentamicin composite coatings that were deposited using matrix-assisted pulsed laser evaporation were shown to possess chemical structures that were similar to those of dropcast coatings[22]. In an *in vitro* study, the gentamicin-containing coatings were shown to inhibit the growth of the gram-positive microorganism *Staphylococcus aureus*.

2. Materials and Methods

2.1 Injection Molding of Microneedle Arrays

The microneedle arrays were prepared using Kuredux® polyglycolic acid (Kureha, Tokyo, Japan) feedstock as previously described[11,12]. Pellets of the polyglycolic acid material were injection-molded with steel molds in a Sesame™ molding machine (Trinks Inc., De Pere, WI, USA) into 1 × 4 microneedle arrays. In the microneedle arrays, the individual microneedles were positioned 1800 µm apart as measured from microneedle center to microneedle center. These injection-molded microneedles were in the form of half-cones on top of a rectangular base; in this array, the faces of the half-cones were aligned with one of the long faces of the rectangular substrate in a co-planar manner.

2.2 Use of Drawing Lithography to Sharpen the Microneedle Tips

A drawing lithography process was used to sharpen the tips of the injection-molded microneedle arrays[11,12]. The microneedles underwent a melt-drawing process, in which the microneedle tips were lowered onto a surface that was heated to a temperature of 220 °C. A servomotor lift platform was used to withdraw the cooling microneedle tips from the stage to create sharp and high aspect ratio tips. The microneedle arrays were placed above a Cimarec™ hotplate (Barnstead International, Dubuque, IA, USA), which was attached to an AVS125 servomotor lift platform (Aerotech Inc., Pittsburgh, PA, USA). The microneedle arrays were positioned such that the half-cone axis was oriented toward the hotplate. When the platform was raised, it made contact with the microneedle tips. The stage was paused for 20 s to melt the microneedle tips; it should be noted that Kuredux® polyglycolic acid exhibits a T_m of 220 °C. The platform was raised by a distance of 550 µm at a rate of 0.5 mm/s. The hotplate was then turned off during a 3 s pause in platform motion. The platform then reversed direction, moving a distance of 1.65 mm at a rate of 1.0 mm/min. When the platform reversed direction, the microneedle tips were drawn into a more tapered structure. The microneedle tips solidified due to the removal of the heat source.

2.3 Nanoindentation of the Uncoated Microneedle

The hardness and reduced modulus values for the base of the uncoated microneedle were obtained using nanoindentation. The microneedle array was attached to a magnetic puck with superglue before the nanoindentation study. The nanoindentation study was carried out using a Hysitron Ubi-1 Nanoindenter; a conical tip was used in this study. Two indentation studies were conducted with a target maximum load of 500 µmol/L. For each test, a loading time of 20 s, a dwell time of 10 s at maximum load, and an unloading time of 20 s were used. The hardness and reduced modulus were calculated from the unloading curves using the Oliver-Pharr approach[23].

2.4 Matrix-Assisted Pulsed Laser Evaporation of Amphotericin B

Solutions containing amphotericin B, polyvinylpyrrolidone, and dimethyl sulfoxide were mixed at room temperature. Polyvinylpyrrolidone and dimethyl sulfoxide are used in topical therapies; for example, polyvinylpyrrolidone is used in microneedles and dimethyl sulfoxide is used in topical preparations that are used to treat fungal nail infections[24,25]. The solutions were prepared by dissolving 1.04 g/mL of amphotericin B or 2.08 g/mL of amphotericin B in dimethyl sulfoxide; it should be noted that all of the final solutions also contained 1 wt% polyvinylpyrrolidone. Prior to each deposition, 3.5 mL of the freshly prepared solution was dropped using a syringe in a copper target holder with a diameter of 3 cm and a height of 5 mm. The solution converted into solid form, which served as the matrix-assisted pulsed laser evaporation target by freezing the solution in liquid nitrogen (77 K) for 30 min. Cryogenesis was achieved by immersing the target in a Dewar vessel that was filled with liquid nitrogen. After freezing, the target holder was quickly mounted in the target position inside the matrix-assisted pulsed laser evaporation chamber.

Amphotericin B coatings were deposited on one-side polished silicon <100> wafer substrates, optic glass substrates, and polyglycolic acid microneedle arrays. The silicon <100> wafer and optic glass substrates were ultrasonically cleaned by immersion in ethanol and drying in air. All of the substrates were sterilized prior to

the matrix-assisted pulsed laser evaporation procedure by exposure to ultraviolet light from a VL-115 UV lamp.

The parameters used for matrix-assisted pulsed laser evaporation of amphotericin B on the surfaces of the silicon <100> wafer substrates, optic glass substrates, and polyglycolic acid microneedles are shown in Table 1. All of the matrix-assisted pulsed laser evaporation depositions were conducted with a KrF* excimer laser source using a wavelength of 248 nm, a repetition rate of 10 Hz, a pulse duration of 25 ns, and an optimum laser fluence of 300 mJ/cm^2; these parameters are commonly used for matrix-assisted pulsed laser evaporation of coatings[26–28]. 150,000 laser pulses were used for each deposition. Both the substrate and the target were rotated at a rate of 50 Hz during the depositions. The laser beam scanned the entire surface of the target at an angle of 45°. During the matrix-assisted pulsed laser evaporation process, the rotating target was maintained in direct contact with a cooling apparatus, which included a liquid nitrogen reservoir and was connected to the target with copper pipes. The target was maintained at a temperature of ~173 K using active liquid nitrogen cooling. Using this setup, rapid evaporation of matrix-assisted pulsed laser evaporation target inside the deposition chamber is significantly decreased. All of the depositions were performed using a background pressure of 2×10^{-1} Pa and a substrate-to-target separation distance of 5 cm. A laser beam homogenizer was used for improving the energy distribution of the laser spot and for increasing the coated region on the substrate.

2.5 Variable Pressure Scanning Electron Microscopy of the Microneedle Arrays

An S-3200 variable-pressure scanning electron microscope with an energy-dispersive X-ray spectrometer (Hitachi, Tokyo, Japan) was used to obtain imaging data and energy-dispersive X-ray spectra from the unmodified and matrix-assisted pulsed laser evaporation-coated microneedle arrays. Prior to imaging, the unmodified and matrix-assisted pulsed laser evaporation-coated microneedle arrays were sputter-coated with a layer of 60% gold–40% palladium for three minutes in a Technics Hummer II system (Anatech, Battle Creek, MI, USA). The energy-dispersive X-ray spectra were obtained in charge reduction mode.

2.6 3D Laser Scanning Confocal Microscopy of the Microneedle Arrays

The surfaces of the unmodified and matrix-assisted pulsed laser evaporation-coated microneedles were evaluated using a VK-X250 3D laser scanning confocal microscope (Keyence, Tokyo, Japan). In this instrument, the laser was rastered in an XY pattern across the field of view, and 0.5 nm steps in the Z-direction were obtained. The 16-bit photomultiplier receiving element was dynamically latched onto the highest reflected laser intensity for each pixel. At that point, it set a color value and height value to create a three-dimensional fully-in-focus topographical map. This laser-based approach enables data acquisition from complex surface shapes.

2.7 Fourier Transform Infrared Spectra of Matrix-Assisted Pulsed Laser Evaporation-Deposited Coatings on Glass

The materials that were processed using matrix-assisted pulsed laser evaporation were examined with Fourier transform infrared spectroscopy to determine if the functional groups of the matrix-assisted pulsed laser evaporation target materials were identifiable in the matrix-assisted pulsed laser evaporation-coated surfaces. The Fourier transform infrared spectra were obtained using a Nexus 470 system, which included an OMNI sampler, a continuum microscope, and OMNIC™ analysis software (Thermo Fisher, Waltham, MA, USA).

2.8 Modified Agar Disk Diffusion Assay of the Microneedle Arrays

A modified agar disk diffusion assay was used to examine the growth-inhibiting effects of (a) the matrix-assisted pulsed laser evaporation-coated microneedle array from deposition with the AmfB(260) target and (b) the matrix-assisted pulsed laser evaporation-coated microneedle array from deposition with the AmfB(520) target; cultures of *Candida albicans* (ATCC 90028) (American Type Culture Collection, Manassas, VA, USA) were used in this study[11,12]. Matrix-assisted pulsed laser evaporation-coated silicon <100> wafer substrates and optic glass substrates were also evaluated in this study. The reagents used for the microbial cultures included yeast nitrogen base, Sabouraud dextrose agar, triphenyltetrazolium chloride, dextrose, and phosphate-

Table 1. The parameters used for matrix-assisted pulsed laser evaporation of amphotericin B onto the surfaces of the polyglycolic acid microneedles. AmfB(260) indicates deposition using a target containing amphotericin B 1040 mg/mL + 1% polyvinylpyrrolidone and AmfB(520) indicates deposition using a target containing amphotericin B 2080 mg/mL + 1% polyvinylpyrrolidone.

Target	T	U (Hz)	Pressure (mbar)	Spot size (mm^2)	Fluence (mJ/cm^2)	Number of pulses	Distance (cm)
AmfB(260)	RT	10	1.6×10^{-2}	30	300	150000	5
AmfB(520)	RT	10	1.6×10^{-2}	30	300	150000	5

buffered saline (10×) (VWR International, West Chester, PA, USA). Overnight broth cultures of *Candida albicans* with yeast nitrogen base and 100 mmol/L dextrose were prepared. Cell pellets were obtained using centrifugation (4500 rpm) for 10 min; these pellets were subsequently resuspended to a cell density of approximately 10^8 cells/mL in phosphate-buffered saline (PBS) (1×); PBS (10×) was diluted using deionized water to create PBS (1×). Agar plates were inoculated with *Candida albicans* cultures following resuspension of the cell pellets. Sabouraud dextrose agar was swabbed with *Candida albicans*. Triphenyltetrazolium chloride was added into each agar plate to serve as a visualization aid; this dye turns red in color in the presence of microbial growth[29–33]. The plates were incubated at 37 °C for 24 hours. After 24 hours, the plates were evaluated for regions of inhibited microbial growth.

2.9 Skin Penetration Properties of the Microneedle Arrays

Discarded human abdominal skin is commonly used to assess the skin penetration properties of microneedle arrays[34]. Methylene blue was used to examine the pores in the human abdominal skin that were created by the microneedle arrays. Surgically discarded human abdominal skin was obtained from Duke Hospital, USA, in accordance with an institutionally approved IRB protocol (DNOR 80 1185-01); the skin was processed with Zimmer Air Dermatome prior to use. The split-thickness skin pieces was preloaded with 200 µL of 1% methylene blue dissolved in water and punched with the uncoated polyglycolic acid microneedle, the matrix-assisted pulsed laser evaporation-coated microneedle from deposition with the AmfB(260) target, or the matrix-assisted pulsed laser evaporation-coated microneedle from deposition with the AmfB(520) target. The microneedle assembly was held using a hemostatic forceps to help control the penetration of the microneedles into the skin. Bright field images were obtained with the Olympus imaging system around 30 min to 1 h after the punch procedure.

3. Results and Discussion

Nanoindentation was used to obtain the hardness and elastic modulus values for the uncoated polyglycolic acid material (Table 2). Taking into account the Poisson's ratio of the diamond indenter tip (0.07) and assuming a Poisson's ratio for the polyglycolic acid material of 0.3, the nanoindentation study indicated that the polyglycolic acid material had a reduced Young's modulus value of approximately 5.5 GPa and a hardness value of approximately 230 MPa. Park *et al.* evaluated the mechanical parameters of microneedle materials and suggested that microneedle materials with Young's modulus values higher than ~1 GPa were associated with fracture forces that surpassed skin insertion forces[35]. The nanoindentation results indicate that the polyglycolic acid material has sufficient stiffness to penetrate the skin.

Table 2. Nanoindentation result obtained from the base of an uncoated polyglycolic acid microneedle. Reduced modulus (E_r) and hardness (H) data were obtained from nanoindentation data using Oliver-Pharr analysis.

Data	Indent 1	Indent 2
Reduced modulus (E_r)	5.61 GPa	5.43 GPa
Hardness (H)	238.96 MPa	217.37 MPa
Maximum depth	287.5 nm	299.1 nm

Figure 2 shows the Fourier transform infrared spectra of matrix-assisted pulsed laser evaporation-deposited coatings on glass. Figure 2(A) shows the spectrum for deposition with the AmfB(260) target (amphotericin B 1040 mg/mL + 1% polyvinylpyrrolidone) and Figure 2(B) shows the spectrum for deposition with the AmfB(520) target (amphotericin B 2080 mg/mL + 1% polyvinylpyrrolidone). The contribution of amphotericin B to the spectra is associated with N–H (overlapped peak around 670 cm^{-1}), C–H (around 750 cm^{-1}), C–O stretching (around 1,380 cm^{-1}), C=C stretching (around 1600 cm^{-1}), C–H stretching (around 3000 cm^{-1}), and O–H stretching (around 3350 cm^{-1})[36]. The contribution of polyvinylpyrrolidone to the spectra is associated with a strong band around 1660 cm^{-1}; this band is assigned to the amide carbonyl group *of N*-vinyl-2-pyrrolidone[37]. Other bands associated with polyvinylpyrrolidone in the spectra are around 1380 cm^{-1}, which is assigned to bond vibrations of the NO_3^- group, and around 1290 cm^{-1}, which is assigned to N–OH bond vibrations[29]. A major absorption band is located at around 1050 cm^{-1}, which is attributed to dimethyl sulfoxide's S–O stretching[37]. The results indicate that the chemical functionality of the matrix-assisted pulsed laser evaporation-deposited coatings is similar to those of the starting materials. The spectral features for the matrix-assisted pulsed laser evaporation-deposited coating do not show a noticeable departure (indicative of chemical modification) from the starting materials.

Figure 3 shows scanning electron microscopy images of unmodified and matrix-assisted pulsed laser evaporation-modified polyglycolic acid microneedles. Figure 3(A–C) show scanning electron micrographs of an uncoated polyglycolic acid microneedle, a scanning electron micrograph of a matrix-assisted pulsed laser evaporation-coated microneedle from deposition with the AmfB(260) target (amphotericin B 1040 mg/mL + 1% polyvinylpyrrolidone), and a scanning electron micrograph of a matrix-assisted pulsed laser evaporation-coated microneedle from deposition with the AmfB(520) target (amphotericin B 2080 mg/mL + 1%

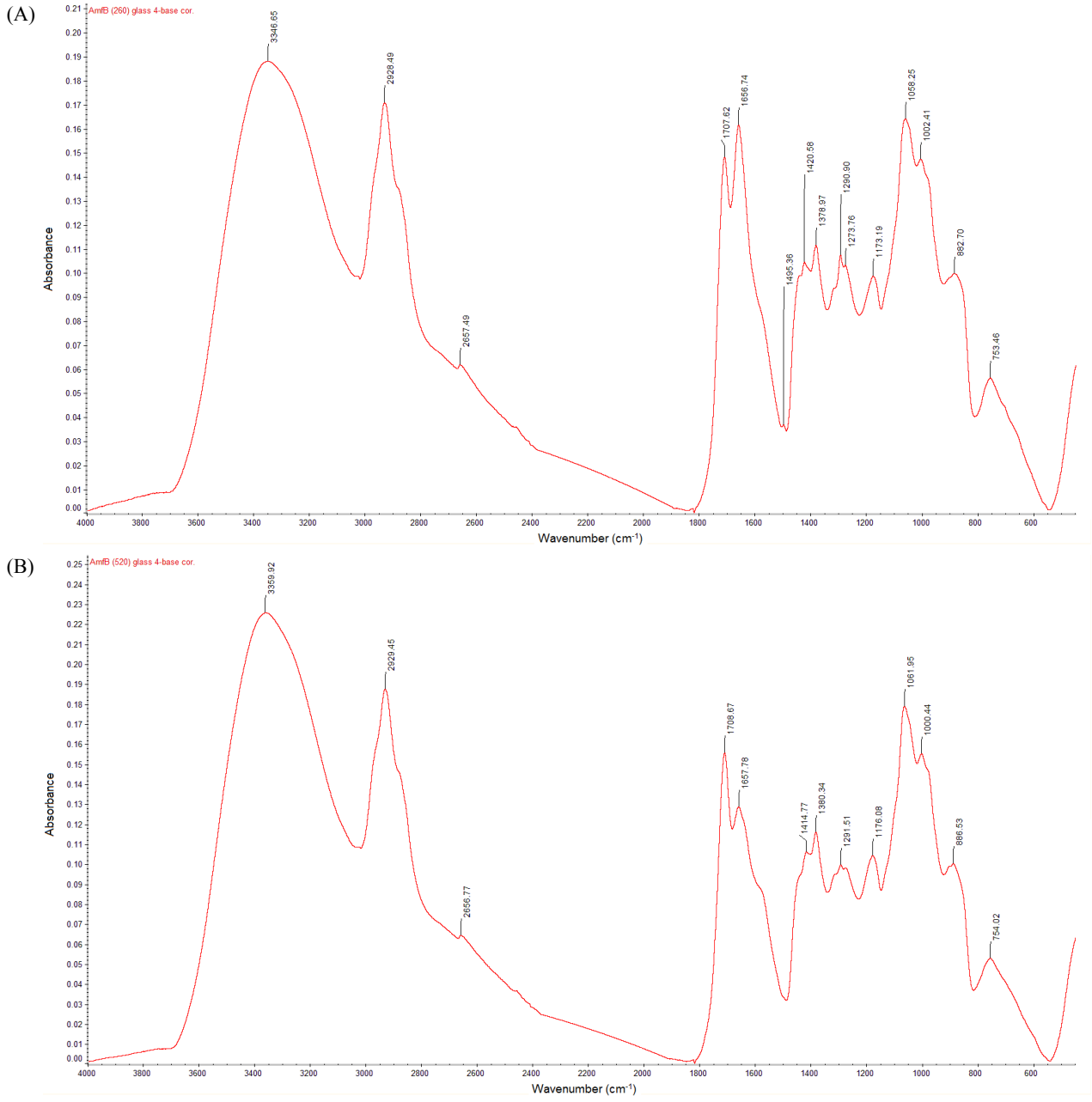

Figure 2. Fourier transform infrared spectra of matrix-assisted pulsed laser evaporation-deposited coatings on glass. Figure (**A**) shows the spectrum for deposition with the AmfB(260) target (amphotericin B 1040 mg/mL + 1% polyvinylpyrrolidone) and Figure (**B**) shows the spectrum for deposition with the AmfB(520) target (amphotericin B 2080 mg/mL + 1% polyvinylpyrrolidone).

polyvinylpyrrolidone), respectively. In previous studies, Boehm *et al.* used the drawing lithography process to create sharpened polyglycolic acid microneedles for tissue penetration[12,13]. As seen in Figure 3(A–C), all of the microneedles created using the combination of injection molding and drawing lithography taper from the base, narrow toward the tip, and come to a point at the tip. In addition, the images of the matrix-assisted pulsed laser evaporation-modified microneedles showed higher surface roughness than the unmodified polyglycolic acid microneedle.

Figure 4(A) shows a 3D representation of an uncoated polyglycolic acid microneedle, Figure 4(B) shows a 3D representation of a matrix-assisted pulsed laser evaporation-coated microneedle from deposition with the AmfB(260) target (amphotericin B 1040 mg/mL + 1% polyvinylpyrrolidone), and Figure 4(C) shows a 3D representation of a matrix-assisted pulsed laser evaporation-coated microneedle from deposition with the AmfB(520) target (amphotericin B 2080 mg/

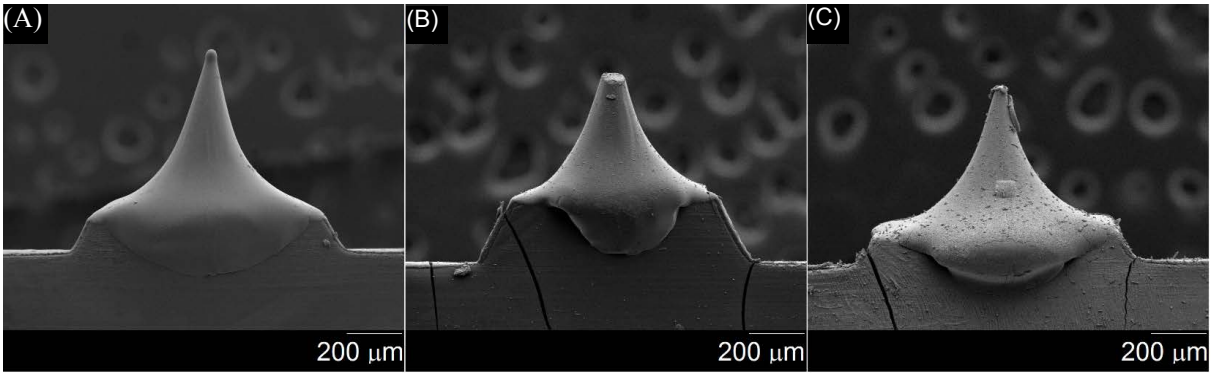

Figure 3. Scanning electron micrographs of (**A**) uncoated polyglycolic acid microneedle, (**B**) matrix-assisted pulsed laser evaporation-coated microneedle from deposition with the AmfB(260) target (amphotericin B 1040 mg/mL + 1% polyvinylpyrrolidone), and (**C**) matrix-assisted pulsed laser evaporation-coated microneedle from deposition with the AmfB(520) target (amphotericin B 2080 mg/mL + 1% polyvinylpyrrolidone).

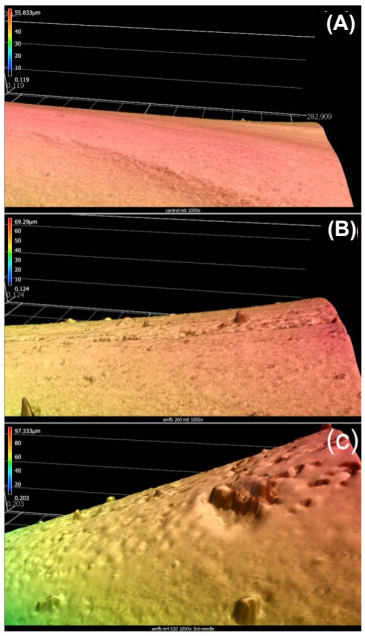

Figure 4. 3D representation of (**A**) uncoated polyglycolic acid microneedle, (**B**) matrix-assisted pulsed laser evaporation-coated microneedle from deposition with the AmfB(260) target (amphotericin B 1040 mg/mL + 1% polyvinylpyrrolidone), and (**C**) matrix-assisted pulsed laser evaporation-coated microneedle from deposition with the AmfB(520) target (amphotericin B 2080 mg/mL + 1% polyvinylpyrrolidone). 3D measurement performed by Keyence VK-X250 Laser Microscope.

mL + 1% polyvinylpyrrolidone). Table 3 shows the R_a (arithmetical mean roughness value), R_z (average maximum height of the profile), RS_m (mean peak width), R_p (maximum profile peak height), R_v (maximum profile valley depth), R_q (root mean square roughness), R_{sk} (skewness), and R_{ku} (kurtosis) values for the unmodified and matrix-assisted pulsed laser evaporation-modified polyglycolic acid microneedles. The R_a value is the oldest and most common roughness parameter in use. It enables one to understand the amplitude of roughness on a profile. The R_a average value is 0.055 μm for the uncoated polyglycolic acid microneedle, 0.122 μm for the matrix-assisted pulsed laser evaporation-coated microneedle from deposition with the AmfB (260) target (amphotericin B 1040 mg/mL + 1% polyvinylpyrrolidone), and 0.251 μm for matrix-assisted pulsed laser evaporation-coated microneedle from deposition with the AmfB(520) target (amphotericin B 2080 mg/mL + 1% polyvinylpyrrolidone). The 3D laser microscopy data indicate that (a) the matrix-assisted pulsed laser evaporation-modified microneedles exhibit higher surface roughness values than the unmodified polyglycolic acid microneedles and that (b) matrix-assisted pulsed laser evaporation targets containing higher drug concentrations produce rougher coatings than matrix-assisted pulsed laser evaporation targets

Table 3. Roughness values obtained from 3D laser microscopy for an uncoated polyglycolic acid microneedle, a matrix-assisted pulsed laser evaporation-coated microneedle from deposition with the AmfB(260) target (amphotericin B 1040 mg/mL + 1% polyvinylpyrrolidone), and a matrix-assisted pulsed laser evaporation-coated microneedle from deposition with the AmfB(520) target (amphotericin B 2080 mg/mL + 1% polyvinylpyrrolidone).

Sample type	Uncoated microneedle	Amf(260) microneedle	Amf(520) microneedle
R_a average (μm)	0.055	0.122	0.251
R_z average (μm)	0.457	0.918	1.564
RS_m average (μm)	4.887	5.853	8.975
R_p average (μm)	0.178	0.487	0.706
R_v average (μm)	0.279	0.43	0.858
R_q average (μm)	0.077	0.173	0.329

containing lower drug concentrations.

Energy-dispersive X-ray spectra of the matrix-assisted pulsed laser evaporation-modified microneedles indicated the presence of carbon, oxygen, and sulfur; the presence of sulfur is associated with the dimethyl sulfoxide solvent that was used to prepare the matrix-assisted pulsed laser evaporation target. Other elements (*e.g.*, elements with known toxicity) were not observed on the surface of the matrix-assisted pulsed laser evaporation-modified microneedles. The unmodified microneedles contained carbon and oxygen; sulfur or other elements were not identified on the surfaces of the unmodified microneedles.

The modified agar diffusion assay result for the unmodified polyglycolic acid microneedle array (which served as a control) shows no inhibition of *Candida albicans* growth. In comparison, the amphotericin B (1040 mg/mL) matrix-assisted pulsed laser evaporation-deposited microneedle array and the amphotericin B (2080 mg/mL) matrix-assisted pulsed laser evaporation-deposited microneedle array show 100% inhibition of *Candida albicans* in zones that measured 11 mm and 18 mm, respectively (Figure 5). The results are comparable to previously reported results, which were obtained from paper disks that were loaded with 10 µg of amphotericin B[38]. The results indicate that matrix-assisted pulsed laser evaporation-modified microneedle arrays successfully delivered amphotericin B to the agar plates, inhibiting the growth of *Candida albicans*. The results for matrix-assisted pulsed laser evaporation-deposited amphotericin B coatings on silicon wafer substrates and glass substrates also showed concentration-dependent activity, with coatings deposited from a 2080 mg/mL target showing higher antifungal activity than coatings deposited from a 1040 mg/mL target (Table 4).

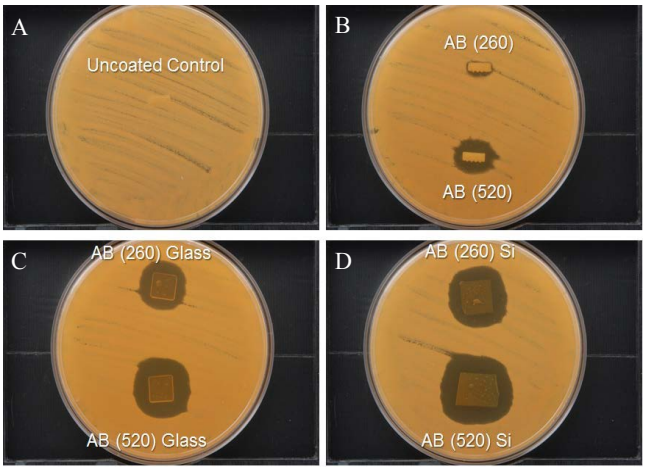

Figure 5. Modified disk diffusion assay result with *Candida albicans* for an uncoated polyglycolic microneedle array (**A**), a matrix-assisted pulsed laser evaporation-coated microneedle array from deposition with the AmfB(260) target (amphotericin B 1040 mg/mL + 1% polyvinylpyrrolidone (noted as AB (260)), and a matrix-assisted pulsed laser evaporation-coated microneedle array from deposition with the AmfB(520) target (amphotericin B 2080 mg/mL + 1% polyvinylpyrrolidone) (noted as AB (520)) (**B**). Zones of growth inhibition were noted surrounding the matrix-assisted pulsed laser evaporation-coated microneedle arrays. In addition, zones of inhibition were noted surrounding pieces of glass (**C**) and silicon (**D**) wafer that were coated with the AmfB(260) target and the AmfB(520) target using matrix-assisted pulsed laser evaporation.

The skin penetration properties of the microneedle arrays were evaluated using methylene blue dye and human skin. Methylene blue was used to visualize the site of microneedle penetration. Figure 6 shows human skin after the application of the microneedle array, removal of the microneedle array, and application of methylene blue. The presence of methylene blue spots in the microneedle array-treated skin indicates that the microneedle arrays are effective in penetrating human skin.

4. Conclusions

The antifungal drug amphotericin B was deposited onto the surfaces of polyglycolic acid microneedles using matrix-assisted pulsed laser evaporation. Solutions containing polyvinylpyrrolidone and amphotericin B in dimethyl sulfoxide were frozen in liquid nitrogen; the solidified solutions were used as targets for matrix-assisted pulsed laser evaporation. Unlike the unmodified microneedles, the matrix-assisted pulsed laser evaporation-coated microneedles exhibited antifungal activity against the yeast *Candida albicans*. The zones of inhibition for the uncoated microneedle array, the amphotericin B (1040 mg/mL) matrix-assisted pulsed laser evaporation-deposited microneedle array, and the amphotericin B (2080 mg/mL) matrix-assisted pulsed

Table 4. Disk diffusion assay data obtained from uncoated and matrix-assisted pulsed laser evaporation-coated surfaces. Data were obtained for an uncoated polyglycolic acid microneedle, a matrix-assisted pulsed laser evaporation-coated microneedle from deposition with the AmfB(260) target (amphotericin B 1040 mg/mL + 1% polyvinylpyrrolidone), and a matrix-assisted pulsed laser evaporation-coated microneedle from deposition with the AmfB(520) target (amphotericin B 2080 mg/mL + 1% polyvinylpyrrolidone). Disk diffusion assay data obtained from matrix-assisted pulsed laser evaporation-coated glass and silicon wafers are also provided.

Sample type	Zone of inhibition (mm)
Control	0
Amf B(260)	11
Amf B(520)	18
Amf B(260) Glass	19
Amf B(520) Glass	24
Amf B(260) Si	25
Amf B(520) Si	31

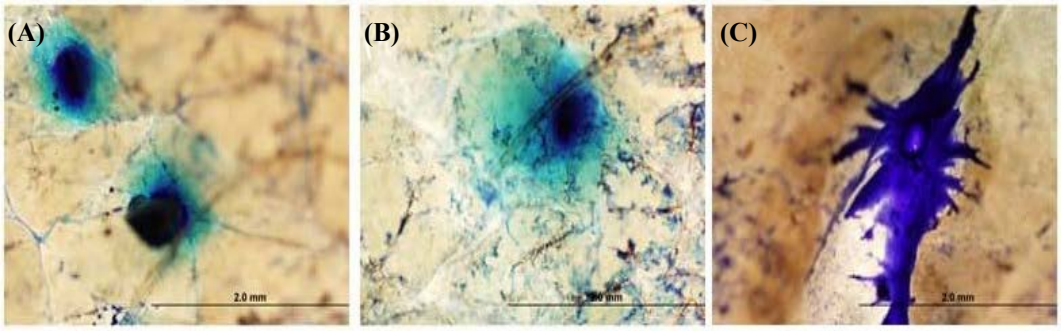

Figure 6. Optical micrographs showing the insertion sites in surgically discarded human abdominal skin for (**A**) an uncoated polyglycolic acid microneedle array, (**B**) a matrix-assisted pulsed laser evaporation-coated microneedle array from deposition with the AmfB(260) target (amphotericin B 1040 mg/mL + 1% polyvinylpyrrolidone), and (**C**) a matrix-assisted pulsed laser evaporation-coated microneedle array from deposition with the AmfB(520) target (amphotericin B 2080 mg/mL + 1% polyvinylpyrrolidone). The location of microneedle insertion was identified using methylene blue dye.

laser evaporation-deposited microneedle array were 0 mm, 11 mm, and 18 mm, respectively. These results suggest that matrix-assisted pulsed laser evaporation may be used to deposit drugs with poor water solubility, such as amphotericin B on the surfaces of microneedles, and that matrix-assisted pulsed laser evaporation-deposited amphotericin B retains pharmacological activity. The matrix-assisted pulsed laser evaporation-coated microneedles containing amphotericin B may have potential use for transdermal treatment of cutaneous Candida yeast infections, other cutaneous fungal infections, and cutaneous parasitic infections. Further studies are needed to assess the dose and exposure time for treatment of fungal and parasitic skin and nail infections.

Conflict of Interest and Funding

No conflict of interest was reported by the authors. We would like to acknowledge C Mooney (NCSU Analytical Instrumentation Facility) for his aid with electron microscopy, B Andersen for her aid with Fourier transform infared spectrosocpy (NCSU College of Textiles), P Strader (NCSU Analytical Instrumentation Facility) for his aid with nanoindentation, the US National Institutes of Health (Award # 1R21AI117748-01A1), the US National Science Foundation (Award CMMI 1258536), and the US Office of Naval Research (Award # N00014-15-1-2323). This work was also supported by the National Program PN 4N/2016(1647-LAPLAS IV and a grant of Ministry of Research and Innovation, CNCS – UEFISCDI, Project Number PN-III-P4-ID-PCE-2016-0884, within PNCDI III.

References

1. Ostrosky-Zeichner L, Marr K A, Rex J H, *et al.*, 2003, Amphotericin B: Time for a new "gold standard". *Clinical Infectious Diseases*, vol.37(3): 415–425. https://dx.doi.org/10.1086/376634
2. Torrado J J, Espada R, Ballesteros M P, *et al.*, 2008, Amphotericin B formulations and drug targeting. *Journal of Pharmaceutical Sciences*, vol.97(7): 2405–2425. https://dx.doi.org/10.1002/jps.21179
3. Trejo W H and Bennett R E, 1963, *Streptomyces nodosus* sp. nov., the amphotericin-producing organism. *Journal of Bacteriology*, vol.85(2): 436–439.
4. Hamill R J, 2013, Amphotericin B formulations: A comparative review of efficacy and toxicity. *Drugs*, vol.73(9): 919–934. https://dx.doi.org/10.1007/s40265-013-0069-4
5. Laniado-Laborin R and Cabrales-Vargas M N, 2009, Amphotericin B: Side effects and toxicity. *Revista Iberoamericana de Micología*, vol.26(4): 223–227. https://dx.doi.org/10.1016/j.riam.2009.06.003
6. Khanna P, Strom J A, Malone J I, *et al.*, 2008, Microneedle-based automated therapy for diabetes mellitus. *Journal of Diabetes Science and Technology*, vol.2(6): 1122–1129. https:/dx./doi.org/10.1177/193229680800200621
7. Baria S H, Gohel M C, Mehta T A, *et al.*, 2011, Microneedles: An emerging transdermal drug delivery system. *Journal of Pharmacology and Pharmacotherapeutics*, vol.64(1): 11–29. https://dx.doi.org/10.1111/j.2042-7158.2011.01369.x
8. Arora A, Prausnitz M R, Mitragotri S, 2008, Micro-scale devices for transdermal drug delivery. *International Journal of Pharmaceutics*, vol.364(2): 227–236. https://dx.doi.org/10.1016/j.ijpharm.2008.08.032
9. Gill H S, Denson D D, Burris B A, *et al.*, 2008, Effect of microneedle design on pain in human volunteers. *The Clinical Journal of Pain*, vol.24(7): 585–594. https://dx.doi.org/10.1097/AJP.0b013e31816778f9

10. Nahar M, Mishra D, Dubey V, *et al.*, 2008, Development, characterization, and toxicity evaluation of amphotericin B–loaded gelatin nanoparticles. *Nanomedicine*, vol.4(3): 252–261.
https://dx.doi.org/10.1016/j.nano.2008.03.007

11. Boehm R D, Miller P R, Schell W A, *et al.*, 2013, Inkjet printing of amphotericin B onto biodegradable microneedles using piezoelectric inkjet printing. *The Journal of The Minerals, Metals & Materials Society*, vol.65(4): 525–533.
https://dx.doi.org/10.1007/s11837-013-0574-7

12. Boehm R D, Daniels J, Stafslien S, *et al.*, 2015, Polyglycolic acid microneedles modified with inkjet-deposited antifungal coatings. *Biointerphases*, vol.10(1): 011004.
https://dx.doi.org/10.1116/1.4913378

13. Boehm R D. Jaipan P, Skoog S A, *et al.*, 2016, Inkjet deposition of itraconazole onto poly(glycolic acid) microneedle arrays. *Biointerphases*, vol.11(1): 011008.
http://dx.doi.org/10.1116/1.4941448

14. Wu P K, Ringeisen B R, Krizman D B, *et al.*, 2003, Laser transfer of biomaterials: Matrix-assisted pulsed laser evaporation (MAPLE) and MAPLE Direct Write. *Review of Scientific Instruments*, vol.74(4): 2546–2557.
http://dx.doi.org/10.1063/1.1544081

15. Schmidmaier G, Wildemann B, Stemberger A, *et al.*, 2001, Biodegradable poly(D,L-Lactide) coating of implants for continuous release of growth factors. *Journal of Biomedical Materials Research (Applied Biomaterials)*, vol.58(4): 449–455.
http://dx.doi.org/10.1002/jbm.1040

16. Kumar N, Langer R S, Domb A J, 2002, Polyanhydrides: An overview. *Advanced Drug Delivery Reviews*, vol.54(7): 889–910.
https://dx.doi.org/10.1016/S0169-409X(02)00050-9

17. Shieh L, Tamada J, Chen I, *et al.*, 1994, Erosion of a new family of biodegradable polyanhydrides. *Journal of Biomedical Materials Research*, vol.28(12): 1465–1475.
https://dx.doi.org/10.1002/jbm.820281212

18. Göpferich A and Tessmar, J, 2002, Polyanhydride degradation and erosion. *Advanced Drug Delivery Reviews*, vol.54(7): 911–931.
https://dx.doi.org/10.1016/S0169-409X(02)00051-0

19. Patz T M, Doraiswamy A, Narayan R J, *et al.*, 2007, Matrix assisted pulsed laser evaporation of biomaterial thin films. *Materials Science and Engineering C*, vol.27(3): 514–522.
https://dx.doi.org/10.1016/j.msec.2006.05.039

20. Iordache F, Grumezescu V, Grumezescu AM, *et al.*, 2015, Gamma-cyclodextrin/usnic acid thin film fabricated by MAPLE for improving the resistance of medical surfaces to *Staphylococcus aureus* colonization. *Applied Surface Science*, vol.336(1): 407–412.
https://dx.doi.org/10.1016/j.apsusc.2015.01.081

21. Cristescu R, Popescu C, Socol G, *et al.*, 2011, Deposition of antibacterial of poly(1,3-bis-(*p*-carboxyphenoxy propane)-*co*-(sebacic anhydride)) 20:80/gentamicin sulfate composite coatings by MAPLE. *Applied Surface Science*, vol.257(12): 5287–5292.
https://dx.doi.org/10.1016/j.apsusc.2010.11.141

22. Cristescu R, Popescu C, Dorcioman G, *et al.*, 2013, Antimicrobial activity of biopolymer-antibiotic thin films fabricated by advanced pulsed laser methods. *Applied Surface Science*, vol.278: 211–213.
https://dx.doi.org/10.1016/j.apsusc.2013.01.062

23. Li X, Gao H, Murphy C J, *et al.*, 2003, Nanoindentation of silver nanowires. *Nano Letters*, vol.3(11): 1495–1498.
https://dx.doi.org/10.1021/nl034525b

24. Machekposhti S A, Soltani M, Najafizadeh P, *et al.*, 2017, Biocompatible polymer microneedle for topical/dermal delivery of tranexamic acid. *Journal of Controlled Release*, vol. 261: 87–92.
https://dx.doi.org/10.1016/j.jconrel.2017.06.016

25. Capriotti K and Capriotti J A, 2015, Onychomycosis treated with a dilute povidone-iodine/dimethyl sulfoxide preparation. *International Medical Case Reports Journal*, vol.8: 231–233.
https://dx.doi.org/10.2147/IMCRJ.S90775

26. Piqué A, 2011, The matrix-assisted pulsed laser evaporation (MAPLE) process: Origins and future directions. *Applied Physics A*, vol.105(3): 517–528.
https://dx.doi.org/10.1007/s00339-011-6594-7

27. Bubb D M, McGill R A, Horwitz J S, *et al.*, 2001, Laser-based processing of polymer nanocomposites for chemical sensing applications. *Journal of Applied Physics*, vol.89(10): 5739–5746.
http://dx.doi.org/10.1063/1.1362405

28. Paun I A, Ion V, Moldovan A, *et al.*, 2012, MAPLE deposition of PEG:PLGA thin films. *Applied Physcia A*, vol.106(1): 197–205.
http://dx.doi.org/10.1007/s00339-011-6548-0

29. Jovanović Ž, Radosavljević A, Šiljegović M, *et al.*, 2012, Structural and optical characteristics of silver/poly(*N*-vinyl-2-pyrrolidone) nanosystems synthesized by γ-irradiation. *Radiation Physics and Chemistry*, vol.81(11): 1720–1728.
https://dx.doi.org/10.1016/j.radphyschem.2012.05.019

30. Majumdar P, Lee E, Gubbins N, *et al.*, 2009, Synthesis and antimicrobial activity of quaternary ammonium-functionalized POSS (Q-POSS) and polysiloxane coatings containing Q-POSS. *Polymer*, vol.50(5): 1124–1133. https://dx.doi.org/10.1016/j.polymer.2009.01.009

31. Narayan R J, Adiga S P, Pellin M J, *et al.*, 2010, Atomic layer deposition of nanoporous biomaterials. *Materials Today*, vol. 13(3): 60–64. https://dx.doi.org/10.1016/S1369-7021(10)70035-3

32. Majumdar P, He J, Lee E, *et al.*, 2010, Antimicrobial activity of polysiloxane coatings containing quaternary ammonium-functionalized polyhedral oligomeric silsesquioxane. *Journal of Coatings Technology and Research*, vol.7(4): 455–467. https://dx.doi.org/10.1007/s11998-009-9197-x

33. Kugel A, Chisholm B, Ebert S, *et al.*, 2010, Antimicrobial polysiloxane polymers and coatings containing pendant levofloxacin. *Polymer Chemistry*, vol.1(4): 442–452. https://dx.doi.org/10.1039/B9PY00309F

34. Gittard S D, Ovsianikov A, Monteiro-Riviere N A, *et al.*, 2009, Fabrication of polymer microneedles using a two-photon polymerization and micromolding process. *Journal of Diabetes Science and Technology*, vol.3(2): 304–311. https://dx.doi.org/10.1177/193229680900300211

35. Park J H, Allen M G, Prausnitz M R, 2005, Biodegradable polymer microneedles: Fabrication, mechanics and transdermal drug delivery. *Journal of Controlled Release*, vol. 104(1): 51–66. https://dx.doi.org/10.1016/j.jconrel.2005.02.002

36. Singh P K, Sah P, Meher J G, *et al.*, 2016, Macrophage-targeted chitosan anchored PLGA nanoparticles bearing doxorubicin and amphotericin B against visceral leishmaniasis. *RSC Advances*, vol.6(75): 71705–71718. https://dx.doi.org/10.1039/C6RA06007B

37. Wallace V M, Dhumal N R, Zehentbauer F M, *et al.*, 2015, Revisiting the aqueous solutions of dimethyl sulfoxide by spectroscopy in the mid- and near-infrared: Experiments and Car–Parrinello simulations. *Journal of Physical Chemistry B*, vol.119(46): 14780–14789. https://dx.doi.org/10.1021/acs.jpcb.5b09196

38. Espinel-Ingroff A, Canton E, Fothergill A, *et al.*, 2011, Quality control guidelines for amphotericin B, itraconazole, posaconazole, and voriconazole disk diffusion susceptibility tests with non-supplemented Mueller-Hinton Agar (CLSI M51-A document) for nondermatophyte filamentous fungi. *Journal of Clinical Microbiology*, vol.49(7): 2568–2572. https://dx.doi.org/10.1128/JCM.00393-11Cae que iunt. Accus